ISSN 0208-7774 TRIBOLOGIA 3/2020 p. 23–31
DOI: 10.5604/01.3001.0014.4754

Joanna KOWALCZYK*

EVALUATION OF TiN COATING PROPERTIES DEPOSITED ON HS6-5-2C STEEL

OCENA WŁAŚCIWOŚCI POWŁOKI TiN OSADZONEJ NA STALI HS6-5-2C

Key words: TiN coating, DLC coating, Al_2O_3, physical vapour deposition PVD.

Abstract: The article presents selected properties of TiN coating on HS6-5-2C steel by Physical Vapour Deposition (PVD). The coating thickness was measured with a Calotest, and its hardness was measured with a nanohardness tester. Tribological parameters were determined, namely, the coefficient of friction and linear wear on the TRB^3 tester operating in a ball-on-disk sliding friction pair. The disc was made of HS6-5-2C steel with a TiN coating and the ball of 100Cr6 steel without coating and with a-C:H coating, with Al_2O_3. The tests were performed under technically dry friction conditions. The coating structure observations were made using a scanning microscope, and the analysis of the geometric structure of samples, before and after tribological tests, were performed with an optical profile measurement gauge. The test results showed that the lowest linear wear was obtained for friction pairs with an Al_2O_3 ball and a steel ball with a-C:H coating applied.

Słowa kluczowe: powłoka TiN, powłoka a-C:H, Al_2O_3, fizyczne osadzanie z fazy gazowej PVD.

Streszczenie: W artykule przedstawiono wybrane właściwości powłoki TiN osadzonej na stali HS6-5-2C techniką fizycznego osadzania z fazy gazowej PVD. Zmierzono grubość powłoki przy użyciu Calotestera oraz jej twardość za pomocą nanotwardościomierza. Określono parametry tribologiczne, a mianowicie współczynnik tarcia i zużycie liniowe na testerze TRB^3 pracującym w skojarzeniu trącym kula–tarcza w ruchu ślizgowym. Tarcza wykonana była ze stali HS6-5-2C z powłoką TiN, a kula ze stali 100Cr6 bez i z naniesioną powłoką a-C:H, z Al_2O_3. Badania wykonano w warunkach tarcia technicznie suchego. Obserwacje struktury powłoki zrealizowano przy użyciu mikroskopu skaningowego, a analizę struktury geometrycznej powierzchni próbek przed i po testach tribologicznych wykonano profilometrem optycznym. Wyniki badań wskazały, że najmniejsze zużycie liniowe uzyskano dla par trących z kulą wykonaną z Al_2O_3 oraz stalową z naniesioną powłoką a-C:H.

INTRODUCTION

As the world economy develops rapidly, the losses caused by friction and wear continue to increase, exacerbating the energy crisis. According to statistical information, about 30% of the world's primary energy resources are consumed by friction and about 80% of mechanical components fail due to wear. Based on different development patterns, friction losses represent on average 2% –7% of GDP annually, which translates into 1.7–6.0 trillion USD worldwide in 2018. For countries with advanced manufacturing industries, such as China, the USA, Germany, and Japan, the friction loss rates may be even higher **[L. 1]**. Holmberg and Erdemir **[L. 2]** reported that about USD 3 trillion is spent on fuel annually. If friction can be reduced by 18%, around USD 90 billion can be saved and CO_2 emissions can be reduced by 290 million tonnes per year, with a significant reduction in PM2.5 emissions. Therefore, the development of new anti-wear technologies has become an important research objective in order to save energy resources, reduce environmental pollution, and improve the ecological environment **[L. 1]**.

An effective way to reduce energy losses and increase the efficiency of the engineering industry is to reduce friction and wear between surfaces in sliding contact. This method is used, not only by the automotive industry, but also in machining **[L. 3]**, namely, the use

* ORCID: 0000-0003-4641-0032. Kielce University of Technology, Faculty of Mechatronics and Mechanical Engineering, Tysiąclecia Państwa Polskiego 7 Ave., 25-314 Kielce, Poland, e-mail: jkowalczyk@tu.kielce.pl.

of thin, hard coatings. An example of such a coating is titanium nitride (TiN), which has a sodium chloride structure. It is a refractory compound with low density (5.22 g/cm^3) and high melting point (2 930°C). TiN has been used since the mid-1960s to coat tool steels. The reason for applying the TiN coating is to increase the durability of, for example, cutting tools, improve the quality of the product surface, and increase the efficiency **[L. 4]**. The advantages of the TiN coating include the following: appearance – golden yellow colour, high hardness (2 400 HV) and adhesion, good ductility, excellent lubricity **[L. 2–3]**, high chemical stability, resistance to wear, corrosion **[L. 4–9]** and high temperature, as well as a low friction coefficient **[L. 4]**.

With the growing popularity of TiN coatings, a great deal of literature on the application process and research and development of coatings has appeared in recent years. Thin TiN films can be applied by Chemical Vapour Deposition (CVD) **[L. 10]** and Physical Vapour Deposition (PVD) **[L. 11, 12]**. The CVD method requires a high temperature (900^{-1} 100°C) **[L. 5, 10]**; therefore, this method is not suitable for tool steels as additional treatments (hardening and tempering) may be necessary to re-harden the base material, which in turn may affect the dimensional tolerance and adhesion of the coating. On the other hand, PVD takes place at much lower temperatures from 200°C to 600°C and therefore are widely applied for tool steels **[L. 5]**.

In the paper **[L. 13]**, the authors tested tribological properties of TiN coating depending on its roughness in a reciprocating motion, where an Al_2O_3 ball was the counter sample. Low friction coefficient values were obtained, which were attributed to the presence of titanium oxide in the wear mark. In addition, it has been proven that the friction coefficient of coatings with high roughness values decreases as the sliding speed increases.

In this article, a TiN coating with a roughness of approx. 80 nm was selected for testing, where the counter sample was a 100Cr6 steel ball, 100Cr6 steel with DLC coating, and Al_2O_3. The tests were performed under technically dry friction conditions.

MATERIALS AND TEST METHODOLOGY

A disc with a diameter of 36 mm and a height of 6 mm made of HS6 5 2C steel was used with a TiN coating applied, and a ball with a diameter of 6 mm made of 100Cr6 steel without coating and with a a-C:H type DLC coating and with Al_2O_3 were used for the tests. Physical Vapour Deposition was applied on the coatings at a temperature of approx. 300°C. HS6-5-2C steel has very good ductility, impact strength, and abrasion resistance. Its chemical composition is listed in **Table 1**. This steel is designed for hot working and can be heat treated at high temperatures. Its hardness after tempering at 500 – 550°C is 65 HRC.

Table 1. Composition of HS6-5-2C steel
Tabela 1. Skład chemiczny stali HS6-5-2C

Element	C	Mn	Si	P	S	Cr	Ni	Mo	W	V	Co	Cu
%	0.82 – 0.92	≥ 0.4	≥ 0.5	≥ 0.03	≥ 0.03	3.5 – 4.5	≥ 0.4	4.5 – 5.5	6 – 7	1.7 – 2.1	≥ 0.5	≥ 0.3

The purpose of the tests was to assess the tribological properties of the TiN coating under technically dry friction conditions in combination with 100Cr6 steel and a-C:H diamond-like coating and Al_2O_3.

The TiN coating thickness was measured with the compact Anton Paar Calotest CATc module**.** The measurement of the nanohardness of the TiN coating was performed using an NHT2 instrumental nanohardness tester from Anton Paar. Using a scanning electron microscope Phenom XL equipped with an EDS microanalyser, the elements contained in the samples used were observed and identified.

Using the confocal microscope with an interferometer mode Leica DCM8, the geometric structure sample surface was measured and analysed before and after the friction tests.

Tribological tests were conducted on a TRB^3 working in the ball-on-disk pair. The tests were conducted with the following parameters:

- Friction combination:
  - HS6-5-2C steel disc with TiN coating – 100Cr6 steel ball;
  - HS6-5-2C steel disc with TiN coating – 100Cr6 steel ball with a-C:H coating;
  - HS6-5-2C steel disc with TiN coating – 2 ball;
- Load P = 10 N;
- Sliding speed v = 0.1 m/s;
- Friction path s = 1000 m;
- Moisture content 30 ± 5%;
- Ambient temperature T_0 = 22±4°C, and
- Lubricants: none – technically dry friction TTS.

TEST RESULTS

The TiN coating thickness of 1.63 μm was measured using a CATc Calotest. Microscopic images and coating thickness measurements are shown in **Figure 1.**

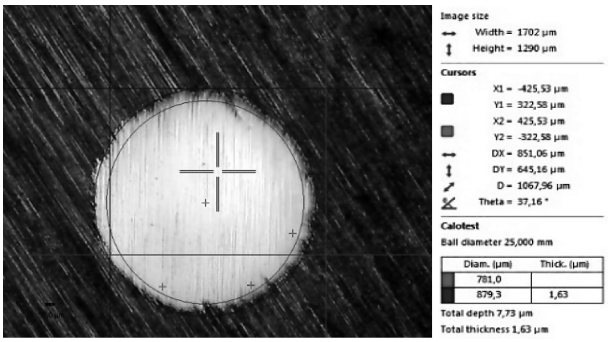

Fig. 1. View of the place of wiping of the coating with a measurement made with an optical measuring system

Rys. 1. Widok miejsca wytarcia powłoki z pomiarem wykonanym optycznym systemem pomiarowym

A microsection was also made, a cross-section was observed, thickness was measured, and a linear distribution of TiN coating elements was prepared (**Fig. 2**).

The thickness of the TiN coating was measured from the cross-section presented above, which was about 1.7 µm (**Fig. 2a**). Comparing the results obtained with the SEM microscope with the thickness measurement on the Calotest CATc, the values obtained are similar (difference 0.07 µm). However, the analysis of linear distribution of elements (**Fig. 2b**) showed the presence of elements such as: titanium and nitrogen.

The measurement of the base nanohardness and the TiN coating were used to determine their hardness, which was 920.37 HV for the base and 1 190.37 HV for the coating, respectively.

Figure 3 illustrates the changes in the force from the penetration depth of the indenter (load-strain curves) and shows the views of imprints after the measurements of the base and TiN coating nanohardness. Analysing the load-strain curves, it was observed that the base and the TiN coating are ductile.

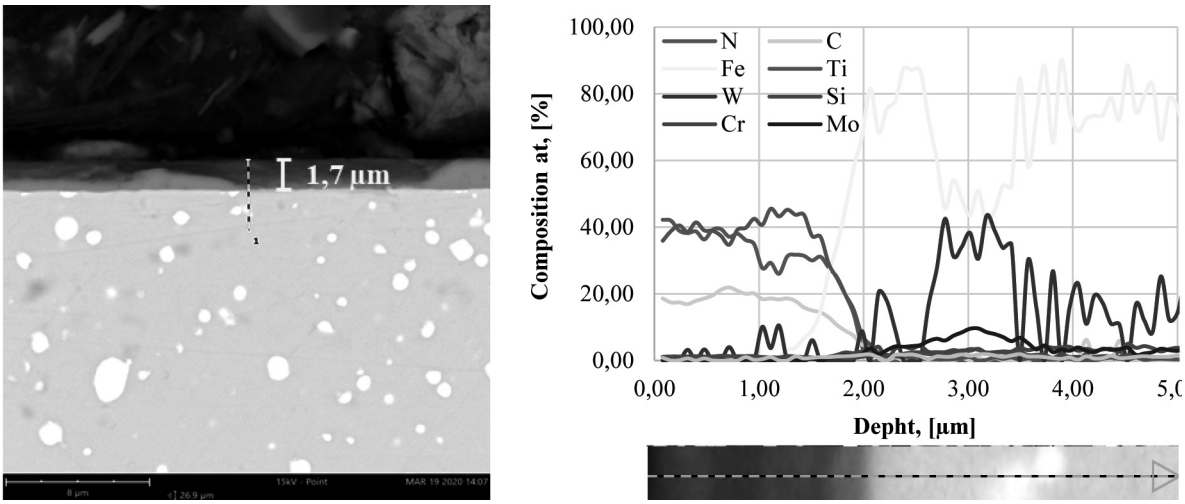

Fig. 2. Results of the linear distribution on the a-C:H coating made on the tested metallographic sample

Rys. 2. Liniowy rozkład pierwiastków powłoki a-C:H wykonany na badanym zgładzie metalograficznym

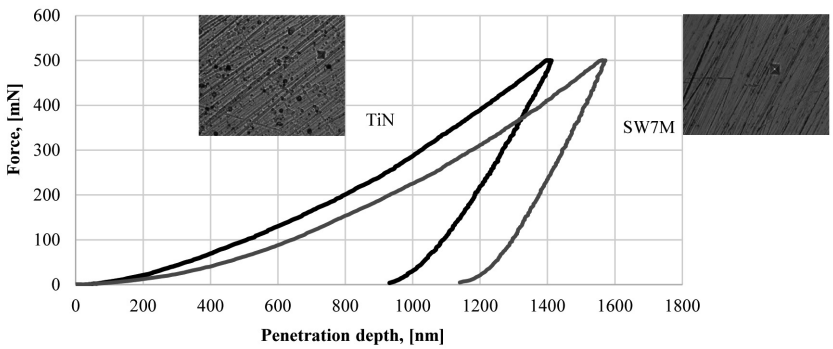

Fig. 3. Graph of force change from the penetration depth of the indenter and view of the impression after the microhardness measurement for the substrate and TiN coating

Rys. 3. Wykres zmiany siły od głębokości penetracji wgłębnika oraz widok odcisku po pomiarze mikrotwardości dla podłoża i powłoki TiN

Before the tribological tests, the geometric structure of the surface of the disc and balls was measured (**Fig. 4**), which was presented as isometric images and primary profiles.

The disc with applied TiN coating (**Fig. 4a**) has a homogeneous surface with small cavities of approx. 40 nm that may have formed during sample preparation. While 100Cr6 steel balls without coating and with DLC and Al_2O_3 coating have a homogeneous structure. The ball with DLC coating (**Fig. 4c**) has small cavities (about 3 µm) visible on the isometric image.

Structure tests with a local analysis of the chemical composition in the micro-area of the TiN coating elements were conducted on a scanning electron microscope equipped with an EDS analyser. The results of these tests are shown in **Figure 5**.

The morphology of the surface of the TiN coating (**Fig. 5a**) shows that the coating has a fairly homogeneous surface with a striped arrangement, which probably results from the preparation of the coating base surface – grinding. Local analysis of the chemical composition of the tested coating showed titanium at 46.96% and nitrogen at 33.40% – from the coating, as well as carbon at 18.68% and silicon at 0.99% from the base material. Whereas, the 100Cr6 steel ball contained

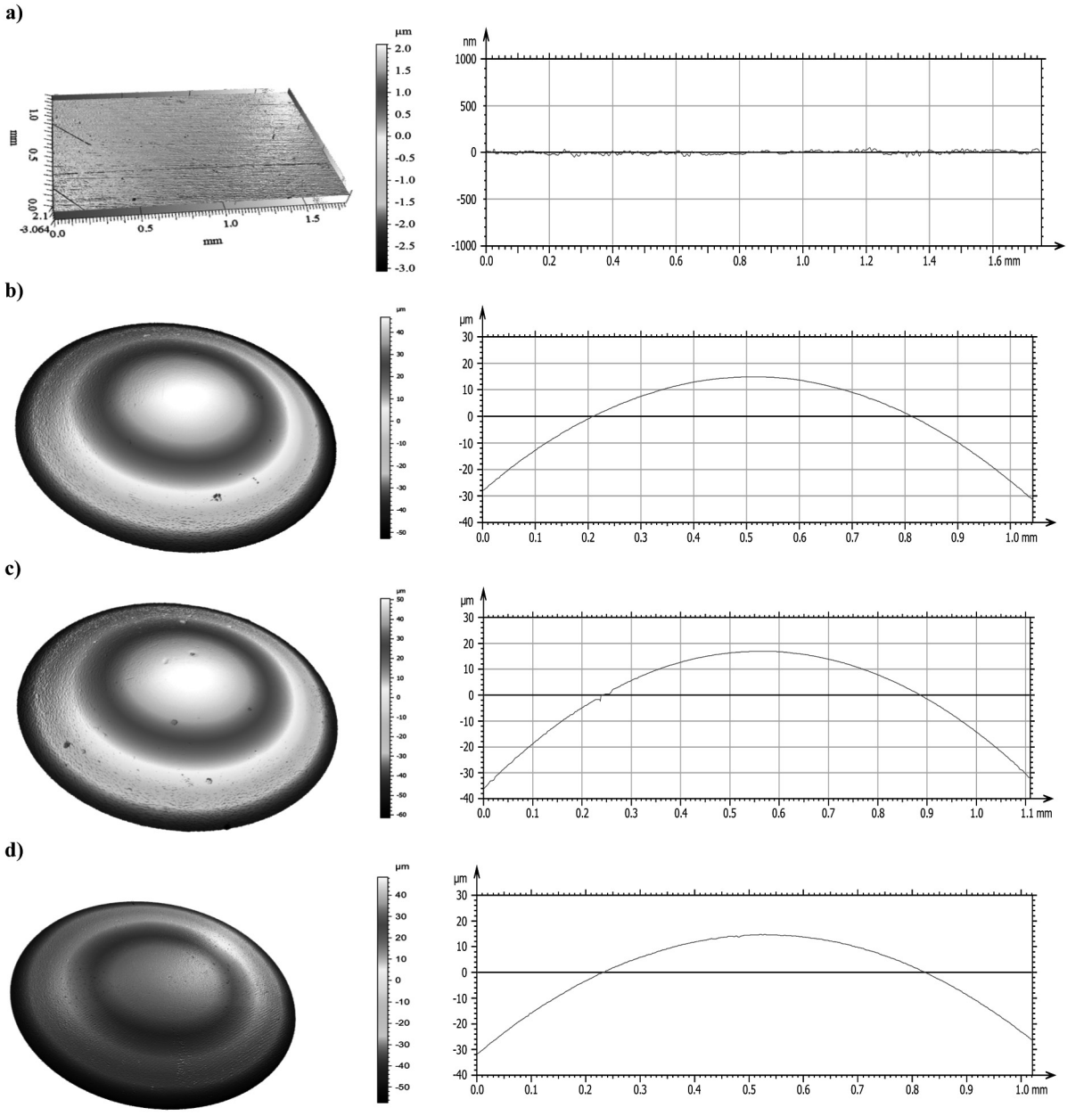

Fig. 4. Isometric views and primary profiles of the samples after the tribological tests: a) disc, b) 100Cr6 steel ball, c) 100Cr6 steel ball with DLC coating, d) Al_2O_3 ball

Rys. 4. Obrazy izometryczne i profile pierwotne próbek przed testami tribologicznymi: a) tarcza, b) kula 100Cr6, c) kula 100Cr6 z powłoką DLC, d) kula z Al_2O_3

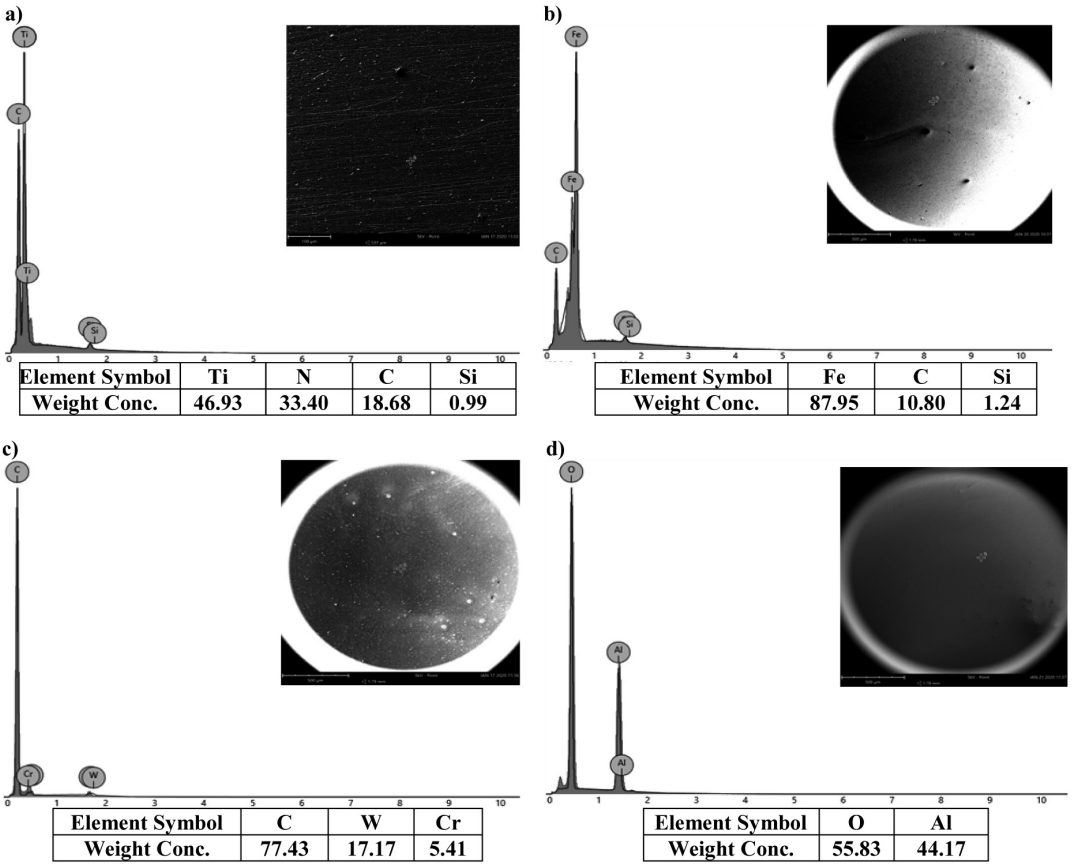

Fig. 5. EDS patterns for different points of the wear track resulting from the sliding contact of the: a) disc, b) 100Cr6 steel ball, c) 100Cr6 steel ball with DLC coating, d) Al_2O_3 ball

Rys. 5. Widmo charakterystycznego promieniowania Rendgenowskiego z obszaru: a) tarczy ze stali HS6-5-2C z powłoką TiN, b) kulą ze stali 100Cr6, c) kulą ze stali 100Cr6 z naniesioną powłoką DLC, d) kulą z Al_2O_3

the following: 87.95% iron, 10.80% carbon, and 1.24% silicon. The ball with DLC coating contained 77.43% carbon, 17.17% tungsten, and 5.41% chromium, which served as the interlayer between the base and the coating. The Al_2O_3 ball has oxygen and aluminium 55.83% and 44.17%, respectively.

Figure 6 shows the results from tribological tests: friction coefficient (**Fig. 6a**) and linear wear (**Fig. 6b**). The lowest friction coefficient value after TTS was observed in combination with a steel ball. The lowest value of linear wear after TTS was recorded after friction in combination with the Al_2O_3 ball and the ball with DLC coating. The TiN coating in frictional contact with the steel ball achieved a friction coefficient that is approximately 33% lower, but approximately 92% higher linear wear than in frictional contact with the Al_2O_3 ball and the DLC-coated steel ball.

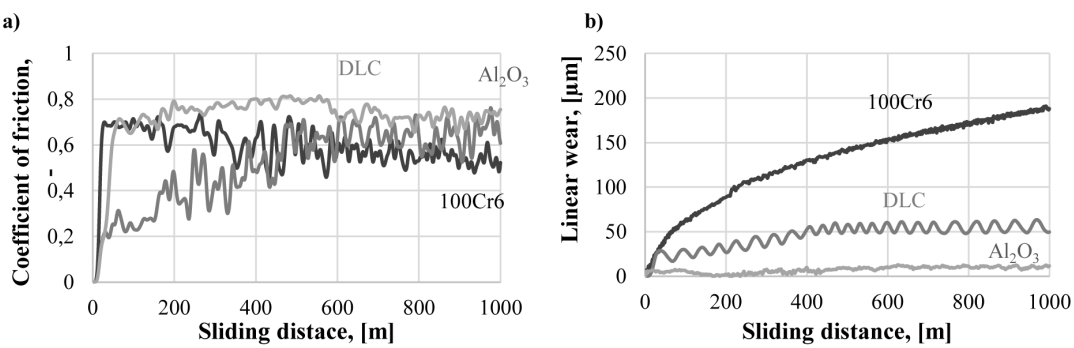

Fig. 6. The graphs: a) coefficient of friction vs. sliding distance, and b) linear wear vs sliding distance

Rys. 6. Wykresy: a) współczynników tarcia oraz b) zużycia liniowego od drogi tarcia

After tribological tests, the samples were observed on a confocal microscope with an interferometric mode. The geometric structure of the sample surface wear marks was analysed (**Fig. 7**) and their maximum depth and area were determined.

By analysing the isometric images and primary profiles of discs, the shallowest depth, the shortest width, and the wear area (**Fig. 7b**) in contact with the DLC-coated steel ball were observed. In turn, the deepest and largest wear area was observed in contact with the Al_2O_3 ball (**Fig. 7c**), although it did not have the widest wear length. This indicates that the ball with Al_2O_3 is harder than the TiN coating. The wear mark is narrow but deep. The widest possible wear trail was obtained after technically dry friction in contact with the steel ball (**Fig. 7a**).

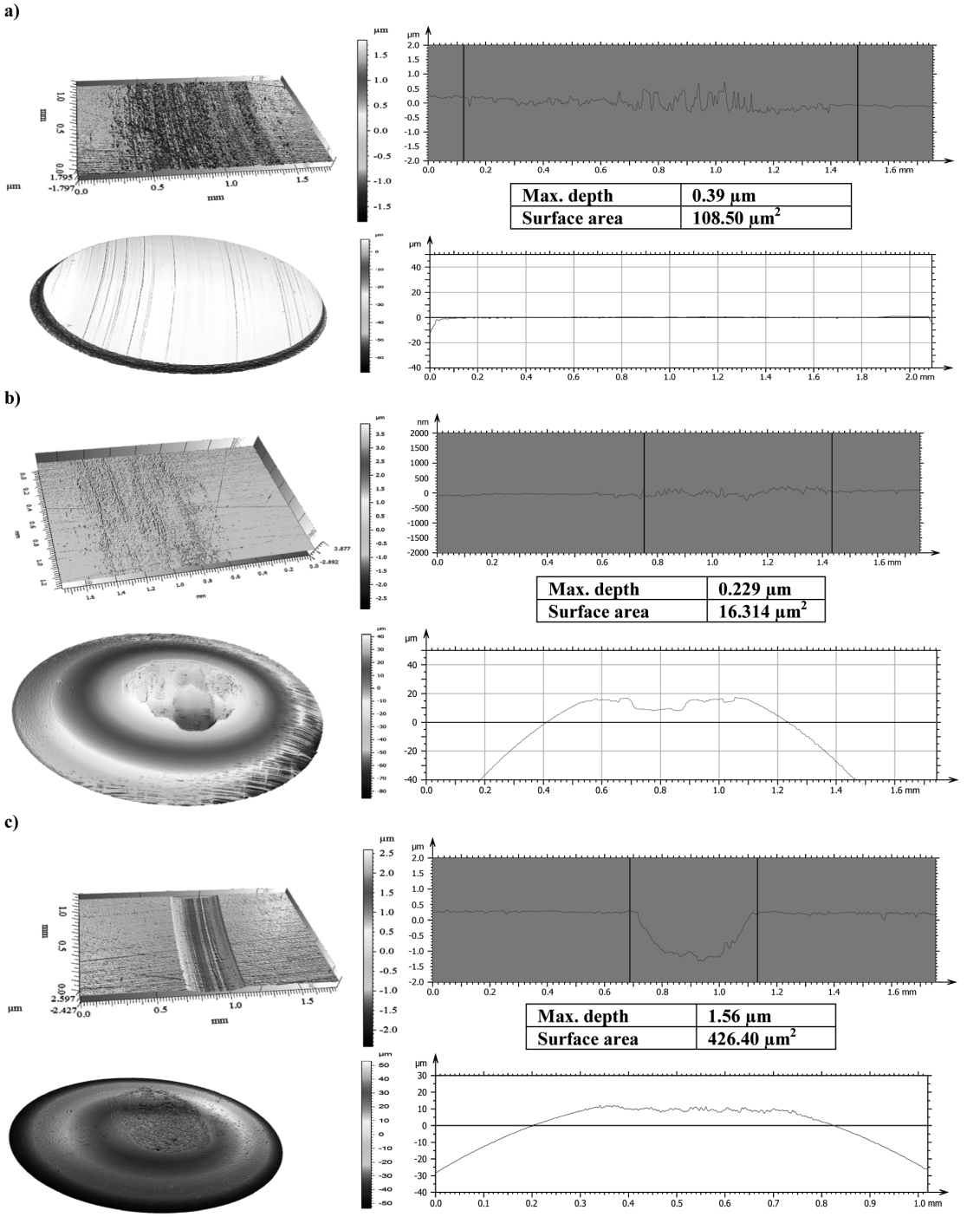

Fig. 7. Isometric views and primary profiles of the discs and balls after the TDF after contact with ball: a) 100Cr6 steel ball, b) 100Cr6 steel ball with DLC coating, c) Al_2O_3 ball

Rys. 7. Obrazy izometryczne i profile pierwotne po TTS w kontakcie z kulą: a) ze stali 100Cr6, b) ze stali 100Cr6 z powłoką DLC, c) z Al_2O_3

Figure 8 shows images of the area in the friction zone together with local analyses of the elemental composition at characteristic spots after tribological tests.

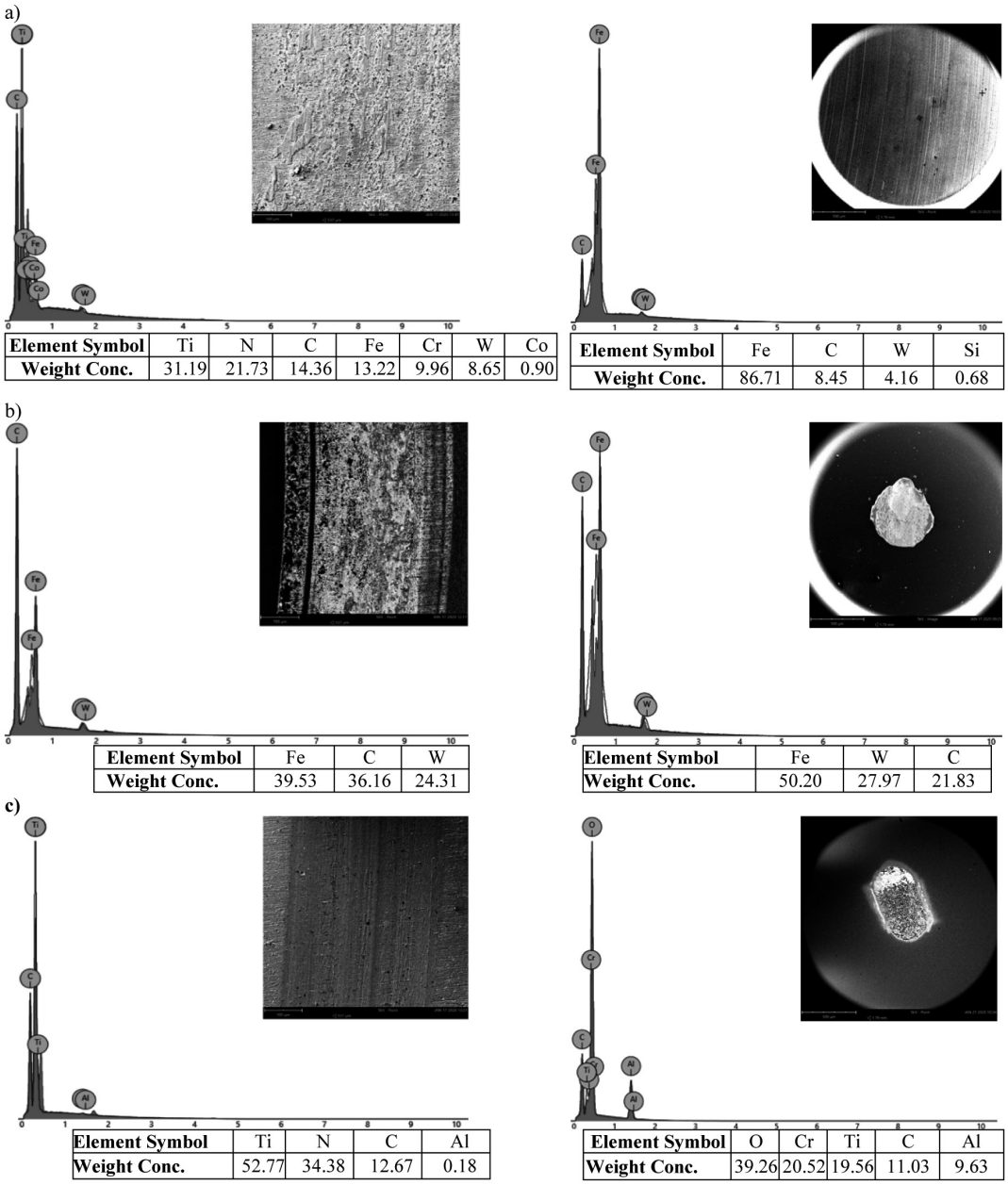

Fig. 8. EDS patterns for different points of the wear track resulting from the sliding contact of the disc after contact with: a) 100Cr6 steel ball, b) 100Cr6 steel ball with DLC coating, c) Al_2O_3 ball

Rys. 8. Widmo charakterystycznego promieniowania Rendgenowskiego z obszaru śladu zużycia tarczy po współpracy tarciowej z kulą: a) ze stali 100Cr6, b) ze stali 100Cr6 z naniesioną powłoką DLC, c) z Al_2O_3

In addition to the coating elements (titanium, nitrogen), the base elements (carbon, iron, chromium, tungsten, cobalt) in the composition of the ball were observed on the disc after technically dry friction TTS in contact with a steel ball (**Fig. 8a**). Elements (tungsten) from the disc were also observed on the ball. After TTS with a ball with DLC coating, the elements of the disc and coating were observed, and, on the ball, in addition to the elements from the coating, an element from the disc (vanadium) was observed. After TTS with the ball with Al_2O_3 on the disc, apart from the elements originating from the disc, additionally aluminium from the ball was observed, which may indicate the formation of titanium oxide, which reduced friction **[L. 13]**.

Table 2 shows the parameters of the geometric structure of the disc and ball surface before and after tribological tests.

Table 2. Surface texture parameters for the: a) discs and b) balls before and after the tribological tests
Tabela 2. Parametry struktury geometrycznej powierzchni: a) tarcz i b) kul przed oraz po testach tribologicznych

a) discs

Surface texture parameters	TiN	TiN – 100Cr6	TiN – a-C:H	TiN – Al_2O_3
Sa[µm]	0.08	0.17	0.55	0.37
Sq[µm]	0.10	0.21	0.69	0.48
Sp[µm]	0.23	1.78	2.54	2.36
Sv [µm]	2.65	2.54	3.39	2.45
Sz[µm]	2.88	4.32	5.93	4.82
Ssk[µm]	–1.69	0.42	–1.19	–1.64
Sku[µm]	43.14	3.81	4.79	4.02

b) balls

Surface texture parameters	100Cr6	a-C:H	Al_2O_3	TiN – 100Cr6	TiN – a-C:H	TiN – Al_2O_3
Sa[µm]	0.10	0.15	0.11	0.09	3.52	0.54
Sq[µm]	0.13	0.50	0.14	0.13	4.52	0.77
Sp[µm]	3.94	0.67	1.14	0.35	10.68	5.89
Sv [µm]	2.43	20.8	1.60	0.85	14.93	3.69
Sz[µm]	6.37	21.45	2.75	1.19	25.61	9.58
Ssk[µm]	–0.59	–28.68	–0.23	–1.98	–0.44	1.03
Sku[µm]	49.55	990.70	3.54	10.37	3.23	6.57

When interpreting the parameters of the geometric structure of the disc surface, the lowest value Sa (arithmetic mean surface height), Sq (square mean surface deviation), Sp (height of the highest surface elevation), Sz (maximum surface height), and Sku (surface slope coefficient or kurtosis) were obtained for the disc in friction combination with a steel ball. This proves that disc surface is smooth, and the lowest values of parameters Sv (depth of the lowest indentation of the surface) and Ssk (coefficient of topography height distribution skewness – surface ordinates) were obtained for the disc in combination with Al_2O_3. The lowest value of the Ssk parameter proves that, as a result of friction, the roughness peaks have disappeared from the disk surface, and single peaks prevail. Such a surface has favourable operating properties, as the lubricant may penetrate the cavities.

In turn, when analysing the parameters of the geometric structure of the balls, the lowest parameter values, i.e. Sa, Sq, Sp, Sv, and Sz, were obtained in the friction combination with the steel ball. This proves the ball surface is smooth. The lowest value of Sku parameter was obtained for a ball with DLC coating and its value was closest to Gaussian distribution (Sku = 3). After the friction with the steel ball, the Ssk parameter had the lowest value, less than zero. This parameter indicates the nature of the surface and the rounding degree of the peaks. The negative value of the Ssk parameter indicates that, as a result of friction, the roughness peaks disappeared from the surface of the steel ball and there are tables and elevations with gentle slopes as well as rounded peaks **[L. 14]**.

CONCLUSIONS

The following conclusions were drawn on the basis of the tests performed:

1. The lowest friction coefficient value was observed after friction combinations with the steel ball.
2. The lowest value of linear wear after TTS was recorded after friction in combination with the Al_2O_3 ball and the ball with DLC coating.
3. The narrowest wear marks were observed for the hardest materials, i.e. those in contact with the ball with DLC coating, and the widest for the softer material, i.e. a steel ball.
4. The TiN coating is hard; therefore, the smallest wear area was obtained in contact with 100Cr6 steel. The clamping of friction pairs occurred here, and the material from the ball entered the build-up composition.
5. It works best with the TiN coating of the ball with DLC and Al_2O_3 coating, because the resulting abrasion is not deeper than the thickness of the coating. The TiN coating did not wear off. In addition, the formation of titanium oxide was observed in contact with the Al_2O_3 ball, which reduced friction.

REFERENCES

1. Luo J., Zhou X.: Superlubricitive engineering – Future industry nearly getting rid of wear and frictional energy consumption. Friction, 2020, 8, 4, pp. 643–665.
2. Holmberg K., Erdemir A.: Influence of tribology on global energy consumption, costs and emissions. Friction, 2017, 5, 3, pp. 263–284.
3. Zaixiu Y., Bhowmick S., Banerji A., Alpas A.T.: Role of Carbon Nanotube Tribolayer Formation on Low Friction and Adhesion of Aluminum Alloys Sliding against CrN. Tribology Letters, 2018, 66, pp. 139.
4. Zhang S., Zhu W.: TiN coating of tool steels: a review. Journal of Materials Processing Technology, 1993, 39, pp. 165–177.
5. Barbosa M. G. C., Viana B. C., Santos F. E. P., Fernandes F., Feitor M. C., Costa T. H. C.: Surface modification of tool steel by cathodic cage TiN deposition. Surface engineering, 2019, 1–9.
6. Song M., Yang Y., Guo J., Xiang M, Zhu O., Ge Y.: A new precursor for fabricating TiN coating on 316L stainless steel at low temperature without corrosive byproducts. Ceramics International, 2019, 45, 15, pp. 18265–18272.
7. Zhao X., Yan D., Li S., Lu C.: The effect of heat treatment on the electrochemical corrosion behavior of reactive plasma-sprayed TiN coatings. Applied Surface Science, 2011, 257, pp. 10078–10083.
8. Mani S.P., Rikhari B., Agilan P., Rajendran N.: Evaluation of the corrosion behavior of a TiN-coated 316L SS bipolar plate using dynamic electrochemical impedance spectroscopy. New Journal of Chemistry, 2018, 42, pp. 14394–14409.
9. Wang H., Zhang R., Yuan Z., Shu X., Liu E., Han Z.: A comparative study of the corrosion performance of titanium (Ti), titanium nitride (TiN), titanium dioxide (TiO2) and nitrogen-doped titanium oxides (N–TiO2), as coatings for biomedical applications. Ceramics International, 2015, 41, pp. 11844–11851.
10. Rebenne H.E., Bhat D.G.: Review of CVD TiN coatings for wear-resistant applications: deposition processes, properties and performance. Surface Coat Technol., 1994, 63, 1, pp. 1–13.
11. Hultman L.: Thermal stability of nitride thin films. Vacuum, 2000, 57, 1, pp. 1–30.
12. Tan C., Zhou K., Kuang T. et al.: Novel performances of in situ plasma nitriding-PVD duplex-treated nanocrystalline TiN coatings. Surface Engineering, 2018, 34, 7, pp. 520–526.
13. Kakaš D., Terek P., Miletić A., Kovačević L., Vilotić M., Škorić B., Krumes D.: Friction and wear of low temperature deposited TiN coating sliding in dry conditions at various speed. Tehnički vjesnik, 2013, 20, 1, pp. 27–33.
14. Niemczewska-Wójcik M., Mańkowska-Snopczyńska A., Piekoszewski W.: Wpływ ukształtowania struktury geometrycznej powierzchni stopu tytanu na charakterystyki tribologiczne polimeru. Tribologia, 2014, 6. pp. 97–112.